STRUCTURE OF ^{26}Na VIA A NOVEL TECHNIQUE USING $(d, p\gamma)$ WITH A RADIOACTIVE ^{25}Na BEAM*

W.N. Catford[a], I.C. Celik[a], G.L. Wilson[a], A. Matta[a]
N.A. Orr[b], C.Aa. Diget[c], P. Adsley[c], H. Al-Falou[d], R. Ashley[e]
R.A.E. Austin[f], G.C. Ball[d], J.C. Blackmon[g], A.J. Boston[e]
H.C. Boston[e], S.M. Brown[a], D.S. Cross[d], M. Djongolov[d]
T.E. Drake[h], U. Hager[d,i], S.P. Fox[c], B.R. Fulton[c], N. Galinski[d]
A.B. Garnsworthy[d], G. Hackman[d], D. Jamieson[j], R. Kanungo[f]
K. Leach[j], J-P. Martin[k], J.N. Orce[d], C.J. Pearson[d]
M. Porter-Peden[i], F. Sarazin[i], S. Sjue[d], C. Sumithrarachchi[d]
C.E. Svensson[j], S. Triambak[d], C. Unsworth[d,e], R. Wadsworth[c]
S.J. Williams[d]

[a]Department of Physics, University of Surrey, Guildford, Surrey GU2 7XH, UK
[b]Laboratoire de Physique Corpusculaire, IN2P3-CNRS, 14050 Caen, France
[c]Department of Physics, University of York, York, YO10 5DD, UK
[d]TRIUMF, 4004 Wesbrook Mall, Vancouver, BC, V6T 2A3, Canada
[e]Department of Physics, University of Liverpool, Liverpool, L69 3BX, UK
[f]Department of Physics, St Mary's University, Halifax, NS, B3H 3C3, Canada
[g]Department of Physics, Louisiana State University, Baton Rouge, USA
[h]Department of Physics, University of Toronto, Toronto, Ontario, Canada
[i]Department of Physics, Colorado School of Mines, Golden, CO 80401, USA
[j]Department of Physics, University of Guelph, Guelph, ON, N1G 2W1, Canada
[k]Département de Physique, Université de Montréal, Montréal, QC, Canada

States in ^{26}Na were populated in the $(d, p\gamma)$ reaction, induced by bombarding deuterium target nuclei with an intense reaccelerated beam of ^{25}Na ions from the ISAC2 accelerator at TRIUMF. Gamma-rays were recorded in coincidence with protons and used to extract differential cross sections for 21 states up to the neutron decay threshold of 5 MeV. Results for levels below 3 MeV are discussed in detail and compared with shell model calculations and with previous work. The angular distributions of decay gamma-rays were measured for individual states and are compared to theoretically calculated distributions, highlighting some issues for future work.

---

* Presented at the Zakopane Conference on Nuclear Physics "Extremes of the Nuclear Landscape", Zakopane, Poland, August 31–September 7, 2014.

1. Introduction and experimental details

The study of spectroscopy in the neutron-rich Ne–Na–Mg region is strongly motivated by the changes in shell structure arising from the monopole interaction between valence nucleons [1–3]. The present study of neutron transfer on to ^{25}Na is motivated by our study of neutron transfer on the isotone ^{24}Ne [4]. That experiment, along with studies using beams of ^{20}O [5, 6] and ^{26}Ne [7] were part of our programme at GANIL/SPIRAL using TIARA [8]. In this study, a ^{25}Na beam was provided by ISAC2/TRIUMF and the silicon array SHARC [9] was used with the germanium clover array TIGRESS [10]. A thin scintillator detector at zero degrees called TRI-FOIL [11] helped to identify and reject background from fusion-evaporation reactions induced on ^{12}C in the 0.5 mg/cm^2 CD$_2$ target. The beam intensity reached 3×10^7 pps, which is 100–1000 times the intensity for our earlier work and is sufficient to allow gating on individual gamma-ray transitions in order to resolve closely spaced levels in the final nucleus. The intensity still falls below the 10^9 pps obtained for ^{19}Ne in the TaLL experiment [12] and this means that gamma–gamma coincidence gating has only limited applicability in the present work. Any particle detected in SHARC triggered the data acquisition, and was then used in the analysis to calculate the excitation energy in ^{26}Na with the assumption that it was a proton from (d, p). Elastic (d, d) scattering was measured simultaneously and provided the absolute normalisation of the cross sections.

2. Results for states in ^{26}Na

The spectrum in figure 1 shows the excitation energy in ^{26}Na, as calculated from the energy and angle of the proton, plotted against the Doppler-corrected energy of coincident gamma-rays. The TRIFOIL requirement has been applied, to reduce background. In figure 2, a region of the gamma-ray energy spectrum is shown, for several slices in excitation energy taken through figure 1. Such spectra allowed a level scheme to be built for ^{26}Na and gamma-decay branching ratios to be determined. Gates on peaks in figure 2 (with appropriate background) allowed the extraction of proton differential cross sections for most states, which, in turn, gave the angular momentum transfer and spectroscopic factors, reported elsewhere [13, 14]. The assignments of J^π values were guided by the excitation energy, the angular momentum transfer, the spectroscopic factor, the comparison with shell model calculations and (importantly) the gamma-ray decay branching ratios. The shell model calculations employed the sd basis with the USD-A interaction [15] for positive parities and a full $1\hbar\omega$ calculation using WBP-M [7] for negative parities. In this work, the additional information that might be available from the gamma-ray angular distributions is also investigated.
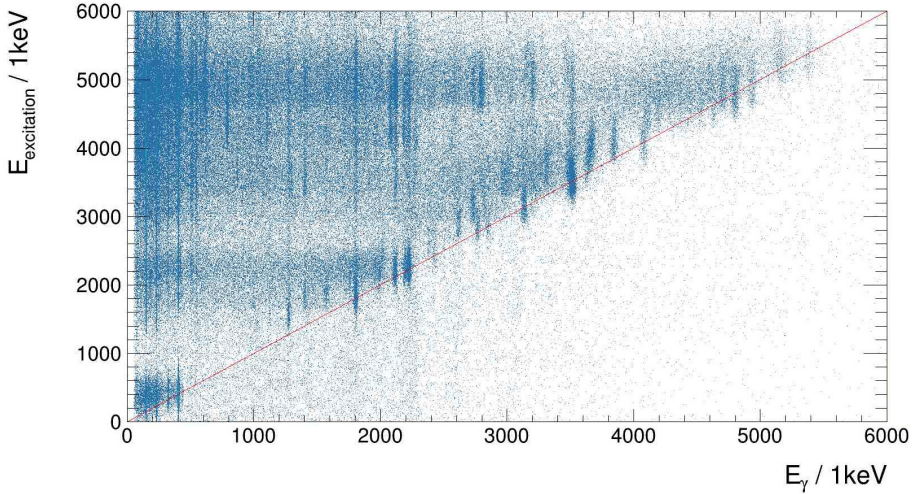
Fig. 1. Excitation energy at which ^{26}Na was populated in the (d, p) reaction, plotted as a function of the Doppler-corrected energy of the recorded gamma-rays. The excitation energy was calculated from the measured energy and angle of the protons observed in the SHARC array. Gamma-ray peaks lying along the diagonal represent decays directly to the ground state.
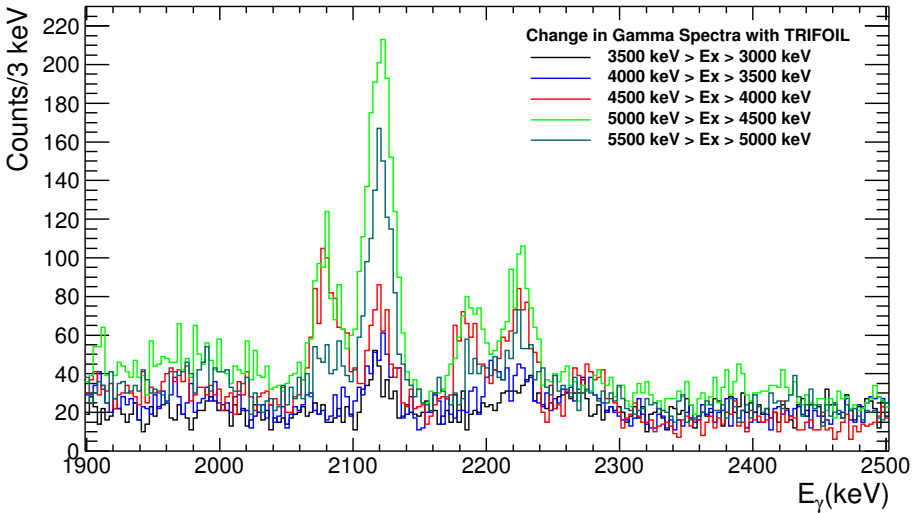

Fig. 2. Example of a region of the Doppler-corrected gamma-ray energy spectrum, showing the effect of different gates placed upon the excitation energy at which the ^{26}Na is populated in the reaction.

The states up to 3 MeV identified in ^{26}Na are compared with previous results and with the shell model in Table I. The lowest energy levels in ^{26}Na may be expected to be dominated by sd configurations. The lowest energy intruder level is the 2^- state which is identified in this work at 2843 keV, and the next is the 3^- at 3135 keV. A one-to-one correspondence is expected between experimental and shell model states, up to 3 MeV (apart from the 2^-). Table I shows that a strict correspondence exists up to the fourth 2^+ state, measured at 2423 keV. The next level is the third 1^+ measured at 2723 keV and populated in β-decay but not transfer. At higher excitations, the density of sd levels becomes higher but the (d,p) selectivity acts to

TABLE I

Excitation energies and identifications of states up to 3 MeV in ^{26}Na, compared with the previous work and with shell model calculations. See the text.

Excitation energy [keV]					Spin
Present	$(^{14}\mathrm{C},d)$ [16]	$(t,^3\mathrm{He})$ [17, 18]	β-decay [19]	Shell	J_i^π
0	0	0	0	0	3_1^+
82.0	82.5	88	82.5	77	1_1^+
232	233	241	233	148	2_1^+
405	406	420	406	416	2_2^+
	1408				
1507	1513		1511	1409	1_2^+
				1522	0_1^+
	1661				
1805		1869		1676	3_2^+
1992	1997	1996		1758	4_1^+
	2046	2048			
2116	2126			2240	5_1^+
	2182	2186			
2194				2142	2_3^+
2225	2232			2048	4_2^+
	2284	2290			
2423				2452	2_4^+
	2454	2456			
	2712	2697	2723	2412	1_3^+
				2600	1_4^+
		2815			
2843				2936	2_1^-
				2930	3_3^+
		2938	2933		

suppress them. Mostly negative parity levels are seen at higher energies in the present work, corresponding to neutron transfer into the fp shell. This is analogous to the behaviour seen in (d, p) using ^{24}Ne projectiles [4]. The highest lying state identified in the present experiment [14] is at 5.3 MeV.

The lowest-lying quartet of states in ^{26}Na can be viewed as the coupling of a neutron in $1s_{1/2}$ to the $5/2^+$ ground state and the nearby $3/2^+$ state in ^{25}Na. The latter ^{25}Na state has the three $0d_{5/2}$ protons recoupled to $3/2^+$ and states built upon this are not strongly populated in (d, p), although the two 2^+ states in the quartet are subject to mixing and share the transfer strength. The 1408 and 1661 keV states reported in fusion-evaporation [16] could, in principle, be candidates for the otherwise unassigned 0^+ state calculated to lie at 1522 keV. However, the 1408 keV level is reported [16] to decay only to the ground state, and there is another 1402 keV gamma-ray seen in the present work which may have caused confusion. Indeed, two different transitions of 1402 keV are seen in the present work. One is a decay to the 407 from the 3^+ state at 1805 keV, which also has a branch of similar intensity with energy 1577 keV and a considerably stronger 1806 keV branch directly to the ground state. A 1577 keV transition is certainly seen in Ref. [16], but it is associated with the decay of the postulated 1661 keV state to 82 keV. The spectrum near 1805 keV is not shown in [16], but it is remarked [16] that the 1805 keV peak was not observed. In any case, Ref. [16] shows an excess of counts at 1408 keV, compared to 1577 keV, and this could not arise from decay of the 1805 keV level. The simplest interpretation, overall, is that the proposed 1661 keV level does not exist and the 1408 keV is a candidate for the otherwise unobserved first 0^+ level.

The 1507 and 1513 keV levels are almost certainly the same state, but the present work does not confirm the existence of the weak decay branch [16] via the 405 keV level. The present 1805 keV state can be associated with that reported with a 60 keV uncertainty in $(t, ^3\text{He})$ at 1860 keV [17, 18]. The 1992 and 1997 keV levels are almost certainly the same state, but whereas the approximately equal decay via gamma rays of 1764 and 1996 keV is confirmed, the 1590 keV branch reported in [16] is ruled out. The state reported at 2046 keV [16] will be discussed below. The 2116 and 2126 keV levels are almost certainly the same state, since each is reported to have the unusual feature (in this region of excitation energy) of decaying exclusively to the ground state. The 2182 and 2194 keV levels cannot be the same state, since the 2182 is reported [16] to decay almost always to the 407 keV state via a 1775 keV gamma ray, whereas the 2194 keV level decays mostly to the ground state with an additional 20% branch to the 232 keV level. The part of the gamma ray spectrum containing 1775 keV is not shown in Ref. [16]. The state at 2225 keV has a 5% branch to the 1805 keV level via a 418 keV gamma-ray and otherwise decays directly to the ground state.

The 2232 keV level has a decay that is consistent with this [16], once the tentative 1996 keV branch is assigned to the 1992 keV decay as discussed above. The state reported at 2284 keV [16] will be discussed below. The levels reported at 2423 and 2454 keV cannot be the same state, as their gamma decays are completely different: the 2423 keV level is seen in the present work to decay 61% via a 2015 keV and 39% via a 2423 keV gamma ray, whereas the 2454 keV level is reported [16] to decay 72% and 28% via 2371 keV and 2044 keV gamma rays respectively. The 2371 keV peak, at least, is clear in Ref. [16] but neither peak is seen in the present work. The levels reported at 2712 [16] and 2723 keV [19] are most likely the same and correspond to the third 1^+ state. The proposed levels at 2046 and 2284 keV, are now discussed. The 2046 is reported to decay approximately equally via gamma rays of 2046 and 1639 keV, which are seen very weakly in the gamma ray spectrum of Ref. [16] but not at all in the present work. The 2284 keV level is reported [16] to decay exclusively to the ground state, but this gamma ray is indistinct in Ref. [16] and is not seen in the present work. In conclusion, the evidence for the states reported in Ref. [16] at 1661, 2046, 2182 and 2284 keV is not strong and the present data provide no additional support for their existence. The 1661 keV has no compelling verification at all and can reasonably be dismissed, while the latter three energies are in remarkable agreement with levels reported in charge exchange. These are peaks 5, 6 and 7 in the only published $(t,^3\text{He})$ spectra [17] and are clearly resolved. Similarly, the weak peak labelled 8 in the charge exchange spectrum [17] is in good agreement with either of the 2423 and 2454 keV levels in Table I.

In summary, of the reported levels below 2723 keV only those at 2046, 2182, 2284 and 2454 keV have no suggested shell model counterpart. Meanwhile, the two remaining states predicted by the shell model below 3000 keV are the fourth 1^+ and third 3^+ states. (In fact, it is either the third or fourth 1^+ state that is missing experimentally, depending on which is associated with the 2723 keV.) The shell model predictions show no evidence for significantly over estimating the excitation energy for any of the levels for which associations have been made. It is, therefore, difficult to explain the origin of any of the four unassigned experimental states below 2723 keV.

3. Gamma-ray angular distributions

A new feature of the present work is that gamma-ray angular distribution measurements have been performed for the nine strongest transitions and compared with predictions based upon the adopted spins. The results are still preliminary but have identified some important issues that are now discussed. In order to predict the gamma-ray angular distribution, the mag-

netic substate populations of ^{26}Na nuclei are calculated within the ADWA model [20] using a code that has been adapted to integrate the substate populations over all azimuthal angles ϕ for the transfer reaction [21]. The SHARC array closely approximates this situation experimentally. The substate distribution, and therefore the angular distribution, depends upon the angle of observation of the proton. For each proton angle, the angular distribution can be calculated using for example the formalism of Ref. [22]. An example is shown in figure 3. Although the ^{26}Na nuclei are travelling only at $\beta \approx 0.10c$, the effect of the angle transformation to the laboratory frame is also clearly evident in these plots.
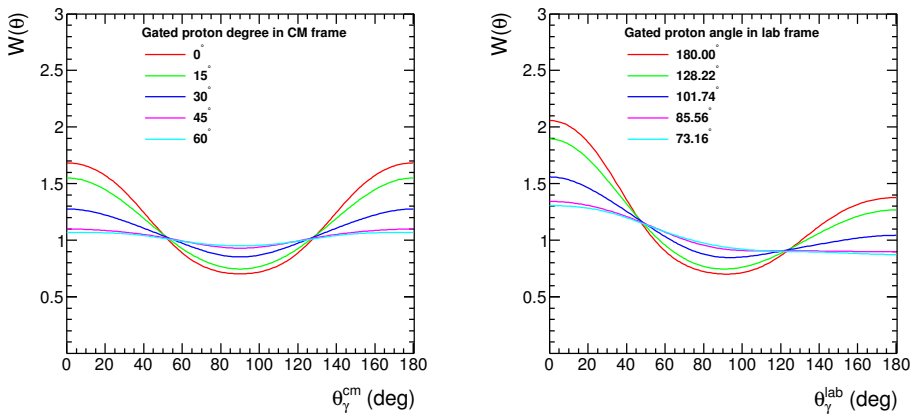

Fig. 3. Gamma-ray angular distributions derived from magnetic substate distributions calculated using ADWA reaction theory: (left) in the rest frame of the ^{26}Na, and (right) in the laboratory frame. The calculation is for the $6^- \rightarrow 5^-$ transition from the state at 4917 keV in ^{26}Na, assumed to be M1. Angles are measured with respect to the beam. Calculations are shown for several different proton angles. The values of the same proton angles are shown as measured (left) in the centre of mass frame for the reaction and (right) in the laboratory frame.

The procedure adopted to average the gamma-ray angular distribution over all proton angles is shown in figure 4 for the same transition as in figure 3. This averaging step is necessary because the statistics that have been acquired are not sufficient to be more exclusive in terms of proton angle. Indeed, it is hard to imagine that many experiments with a radioactive beam could ever achieve sufficient statistics for such an analysis. In figure 4, the angle spectrum of observed protons is shown at top left. These proton data were combined with solid angle information in other parts of the analysis to give differential cross sections, but here it is simply the distribution of counts as a function of angle that is used. For the full range of proton angles, the different gamma-ray angular distributions are also plotted, both in the ^{26}Na

rest frame and in the laboratory frame. The averaged distribution, weighted according to the number of protons recorded, is seen to have a less distinct structure compared to most distributions within the range averaged.
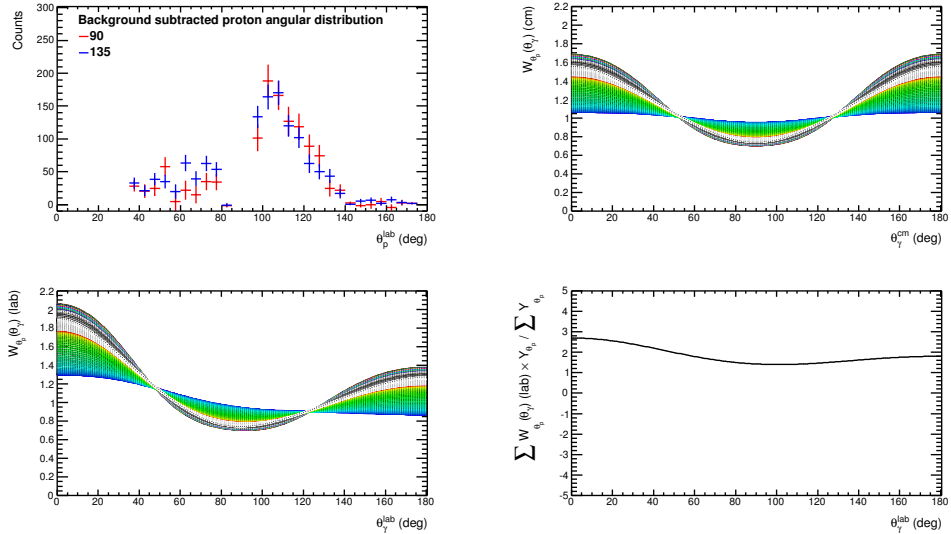

Fig. 4. Sequence of plots showing the calculation of the averaged gamma-ray angular distribution: (top left) the spectrum of laboratory angles for protons populating the 6^- state, (top right) the calculated gamma-ray angular distributions measured in the rest frame of the ^{26}Na for all of these different proton angles, (bottom left) the gamma-ray angular distributions transformed into the laboratory frame, and (bottom right) the weighted average of the gamma-ray angular distributions, weighted according to the number of protons detected at each angle.

The predicted angular distributions for gamma-rays are, of course, model dependent. However, for the transfers that populate the states at 232 and 405 keV in ^{26}Na, the measured differential cross sections show that they are clearly s-wave dominated. The transferred $s_{1/2}$ neutron cannot polarize the ^{26}Na, and so the gamma-ray emission must be isotropic in the rest frame of the ^{26}Na. For these two cases, shown in the top row of figure 5, the data and the calculation show reasonable agreement. The eight data points were obtained by using the electronic segmentation of the TIGRESS clovers [10], which were centred at laboratory angles of 90° (four clovers) and 135° (four clovers). Two more examples are included in figure 5. At bottom left, the transition from the 4087 keV 2^- state to the 1805 keV 3^+ state is shown (assumed to be pure E1 based on systematics in this mass region). The distribution at bottom right is for the $6^- \rightarrow 5^-$ transition from 4917 keV to 4305 keV, assumed to be pure M1 (and discussed in the two

preceding figures). In each case, the experimental distribution appears to be different to the prediction and also it shows more structure. Different spin assumptions do not improve the agreement with the data, so the reason for this discrepancy remains unidentified at this stage.
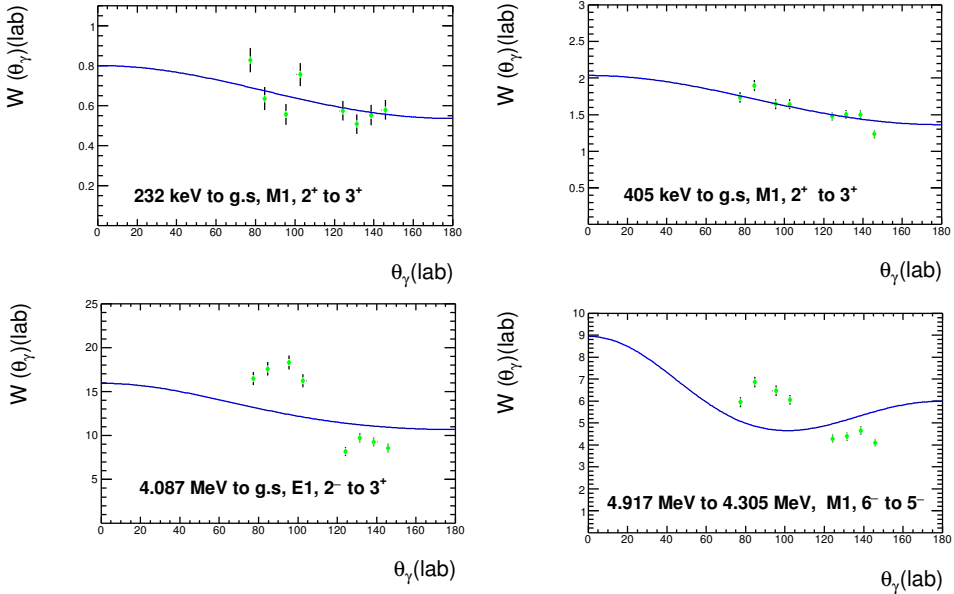

Fig. 5. Experimental data compared to the angle-averaged gamma-ray distributions according to the reaction calculations, for four different transitions in ^{26}Na. The top two cases must be isotropic because the neutron transfer in (d, p) is of an s-wave neutron, and the distorted shape of the theoretical curve simply reflects the Lorentz boost. The two isotropic cases show reasonable agreement between theory and experiment.

4. Conclusions and perspective

The present experiment represents a new approach in which gamma-ray gating has been used to extract differential reaction cross sections for individual states populated in transfer. The details of the analysis are given elsewhere [13, 14] and further issues relating to the experiment and the analysis are discussed in Ref. [23]. Here, the emphasis has been on the comparison with previous work (for states up to 3 MeV in ^{26}Na) and on the recent extension to include the analysis of gamma-ray angular distributions. In principle, angular distributions should allow the multipolarity of gamma-ray transitions to be determined, which will assist in the assignment of spins in this type of study. The need to analyse all proton angles together, due

to the limited statistics achievable, is shown to dilute the angular structure that is expected to be found inherently in the data. This highlights the need for new methods of analysis to be developed, in which the spin information held in the gamma-ray angular distributions for all proton angles can be combined in a constructive fashion.

REFERENCES

[1] T. Otsuka *et al.*, *Phys. Rev. Lett.* **87**, 082502 (2001).

[2] T. Otsuka *et al.*, *Phys. Rev. Lett.* **95**, 232502 (2005).

[3] O. Sorlin, M.-G. Porquet, *Phys. Scr.* **T152**, 014003 (2013).

[4] W.N. Catford *et al.*, *Phys. Rev. Lett.* **104**, 192501 (2010).

[5] B. Fernández-Domínguez *et al.*, *Phys. Rev.* **C84**, 011301(R) (2011).

[6] A. Ramus *et al.*, *Int. J. Mod. Phys.* **E18**, 1 (2009).

[7] S.M. Brown *et al.*, *Phys. Rev.* **C85**, 011302(R) (2012).

[8] M. Labiche *et al.*, *Nucl. Instrum. Methods Phys. Res.* **A614**, 439 (2010).

[9] C.Aa. Diget *et al.*, *J. Inst.* **6**, P02005 (2011).

[10] M.A. Schumaker, C.E. Svensson, *Nucl. Instrum. Methods Phys. Res.* **A575**, 421 (2007).

[11] G.L. Wilson *et al.*, *J. Phys. Conf. Ser.* **381**, 012097 (2012).

[12] W.N. Catford *et al.*, *Nucl. Instrum. Methods Phys. Res.* **A371**, 449 (1996).

[13] G.L. Wilson, Ph.D. Thesis, University of Surrey, 2012, available online at http://epubs.surrey.ac.uk/775380/

[14] I.C. Celik, Ph.D. Thesis, University of Surrey, 2014.

[15] B.A. Brown, W.A. Richter, *Phys. Rev.* **C74**, 034315 (2006).

[16] S. Lee *et al.*, *Phys. Rev.* **C73**, 044321 (2006).

[17] E.R. Flynn, J.D. Garrett, *Phys. Rev.* **C9**, 210 (1974).

[18] N.M. Clarke, K.I. Pearce, *J. Phys. G* **15**, L249 (1989).

[19] L. Weissman *et al.*, *Phys. Rev.* **C70**, 057306 (2004).

[20] R.C. Johnson, P.J. Soper, *Phys. Rev.* **C1**, 976 (1970).

[21] J.A. Tostevin, M. Toyama, M. Igarashi, N. Kishida, Surrey version of the code TWOFNR, http://www.nucleartheory.net/NPG/code.htm

[22] H.J. Rose, D.M. Brink, *Rev. Mod. Phys.* **39**, 306 (1967).

[23] W.N. Catford, *Lect. Notes Phys.* **879**, 67 (2014).